

RESEARCH

Open Access



Nitric oxide donor sodium nitroprusside-induced transcriptional changes and hypocrellin biosynthesis of *Shiraia* sp. S9

Yan Jun Ma^{1,2}, Xin Ping Li¹, Yue Wang¹ and Jian Wen Wang^{1*}

Abstract

Background: Nitric oxide (NO) is a ubiquitous signaling mediator in various physiological processes. However, there are less reports concerning the effects of NO on fungal secondary metabolites. Hypocrellins are effective anticancer photodynamic therapy (PDT) agents from fungal perylenequinone pigments of *Shiraia*. NO donor sodium nitroprusside (SNP) was used as a chemical elicitor to promote hypocrellin biosynthesis in *Shiraia* mycelium cultures.

Results: SNP application at 0.01–0.20 mM was found to stimulate significantly fungal production of perylenequinones including hypocrellin A (HA) and elsinochrome A (EA). SNP application could not only enhance HA content by 178.96% in mycelia, but also stimulate its efflux to the medium. After 4 days of SNP application at 0.02 mM, the highest total production (110.34 mg/L) of HA was achieved without any growth suppression. SNP released NO in mycelia and acted as a pro-oxidant, thereby up-regulating the gene expression and activity of reactive oxygen species (ROS) generating NADPH oxidase (NOX) and antioxidant enzymes, leading to the increased levels of superoxide anion (O_2^-) and hydrogen peroxide (H_2O_2). Gene ontology (GO) analysis revealed that SNP treatment could up-regulate biosynthetic genes for hypocrellins and activate the transporter protein major facilitator superfamily (MFS) for the exudation. Moreover, SNP treatment increased the proportion of total unsaturated fatty acids in the hypha membranes and enhanced membrane permeability. Our results indicated both cellular biosynthesis of HA and its secretion could contribute to HA production induced by SNP.

Conclusions: The results of this study provide a valuable strategy for large-scale hypocrellin production and can facilitate further understanding and exploration of NO signaling in the biosynthesis of the important fungal metabolites.

Keywords: *Shiraia*, Sodium nitroprusside, Nitric oxide, Hypocrellin, Oxidative stress

Background

Shiraia bambusicola P. Hennings is a bambusicolous fungus parasitized on bamboo tender twigs and its fruiting bodies have been used in traditional Chinese medicine to stimulate blood circulation, relieve expectation, cure rheumatism and relax muscle rigidity [1, 2]. Hypocrellins, main perylenequinone pigments

isolated from the hypha and fruit-bodies of *Shiraia* fungi, have been developed as new non-porphyrin and reactive oxygen species (ROS)-generating photosensitizers in photodynamic therapy (PDT) for clinical application of anti-microbes, -cancers and -viruses [1, 3, 4]. Due to the difficulty of chemical synthesis of hypocrellins and the scarcity of wild fruiting bodies [5], *Shiraia* mycelium culture has become a promising production process of this new PDT agent [6]. More process strategies were applied to enhance hypocrellin production in the culture, including the condition optimization for the cultures [7], and application of

*Correspondence: jwwang@suda.edu.cn; bcjwwang@gmail.com

¹ College of Pharmaceutical Sciences, Soochow University, Suzhou 215123, China

Full list of author information is available at the end of the article



biotic [8, 9] or abiotic elicitors [10, 11]. Nitric oxide (NO), a small molecular signal, was found to be involved in the induced hypocrellin production by a fungal elicitor from *Aspergillus niger* at 50 µg/mL [12] and a fungal elicitor PB90 at 5 nM [8]. The endogenous NO in *S. bambusicola* was also observed in extractive culture of *Shiraia* by Triton X-100 [13].

NO is an important regulatory molecule in mammals [14]. Recently, NO has been proved to be an essential signal in the elicitation of plant defense and secondary metabolite biosynthesis [15]. NO released by a NO donor sodium nitroprusside (SNP) could elicit plant secondary metabolites such as marjoram essential oil [16], total phenols and flavonoids in *Echinacea purpurea* roots [17], artemisinin in *Artemisia annua* hairy roots [18], and taxol in *Taxus yunnanensis* cells [19]. However, there are few reports on the effects of NO on fungal growth and secondary metabolism. NO may mediate L-arginine-induced conidiation of *Coniothyrium minitans* [20]. Wang and Higgins (2005) reported that the germination and development of *Colletotrichum coccodes* conidia were significantly inhibited by SNP at 100 µM [21]. A NO-releasing compound diethylenetriamine-NoNoate at 1.5 mM increased drastically the formation of cleistothecia in *A. nidulans*, suggesting a positive regulator of NO on fungal sexual development [22]. Zhao et al. demonstrated that NO was involved in the co-culture of *Inonotus obliquus* with *Phellinus morii* and triggered the biosynthetic pathway of phenylpropanoids, leading to an increased production of styrylpyrone derivatives [23]. SNP at 5 mM increased yield of ganoderic triterpenoid by 40.94% in submerged fermenting *Ganoderma lucidum* [24]. Although the endogenous NO generation was observed in *S. bambusicola* treated by fungal elicitors [8, 12] and Triton X-100 [13], the regulation roles of NO on fungal hypocrellin biosynthesis are still undetermined. Therefore, as a follow-up to our efforts on enhancing hypocrellin production [9, 25] and elucidating the role of NO on secondary metabolite biosynthesis [13, 26], we examined the effects of SNP on *Shiraia* hypocrellin biosynthesis. We also investigated the relationship between NO and elicitation responses including ROS generation, the activation of antioxidant defenses and hypocrellin production in *Shiraia* mycelium cultures. In this study, de novo transcriptome sequencing for *Shiraia* sp. S9 was performed for better understanding the NO regulation on hypocrellin biosynthesis. This study presented a novel elicitor of hypocrellin production and shed light on the relational roles of NO on the biosynthesis of secondary metabolites.

Results

SNP application released NO and enhanced hypocrellin production

After the application of SNP at 0.10 mM to 3-day-old cultures, we observed a rise of green fluorescence of NO indicator 4, 5-diaminofluorescein diacetate (DAF-2-DA) in *Shiraia* mycelia, whereas the relative fluorescent ration was markedly decreased by NO scavenger 2-(4-carboxyphenyl)-4, 4, 5, 5-tetramethylimidazoline-1-oxyl-3-oxide (cPTIO), indicating the release of NO in hyphae (Fig. 1a, b). On the solid medium, the concentration of fungal conidia was decreased from 17.08×10^6 to 2.43×10^6 spores/mL by SNP treatment (Fig. 2a). The pycnidium formation was suppressed by SNP (Fig. 2b). Although SNP at higher concentration (1.00 mM) inhibited the fungal growth, the diameter of fungal colony was increased on day 6 by SNP at 0.01 or 0.02 mM (Fig. 2c, d). In the liquid culture, there were not any notable changes in fungal biomass (Additional file 1: Figure S1A), pH value and sugar consumption (Additional file 1: Figure S2) in medium after SNP application at 0.10 mM. However, SNP decreased fungal pellet diameter by 16.09–25.73% (Additional file 1: Figure S1B) and the pellets were colored with dark red (Fig. 2e). The influence of SNP on hypocrellins including hypocrellin A (HA) and HC, and elsinochrome (A, B and C) in the culture was detected by HPLC (Additional file 1: Figure S3). Both the intracellular HA (1.22-fold of control) and EA (5.88-fold of control) were enhanced by SNP at 0.10 mM (Table 1). The extracellular HA was increased by 87.56%, while HC, EB and EC were not detected in cultural broth with or without SNP treatment.

As HA is a major bioactive hypocrellin constituent in *Shiraia* [9], we optimized the conditions (concentration and addition time) of SNP application to obtain higher HA production. SNP at lower concentrations (0.01–0.20 mM) had no obvious impacts on fungal biomass (Additional file 1: Figure S4A), but increased HA contents in mycelium and in cultural broth. The higher HA in mycelium (9.72 mg/g DW) and in cultural broth (4.64 mg/L) were obtained at 0.02 mM and 0.20 mM, respectively (Additional file 1: Figure S4B, C). When SNP at 0.02 mM was applied on different days, the higher contents of intracellular HA (9.97 mg/g DW) and the released HA in cultural broth (4.42 mg/L) were achieved on day 3 (Additional file 1: Figure S5). Hence, SNP application at 0.02 mM on day 3 of the culture was then used for subsequent culture. The time course of the effect of SNP on HA production in 9-day-old cultures was shown in Fig. 3. Under this optimal condition, SNP application did not suppress mycelial growth (Fig. 3a), but promoted the intracellular HA contents by 73.31–178.96% (Fig. 3b) and extracellular HA accumulation by 26.09–119.26%

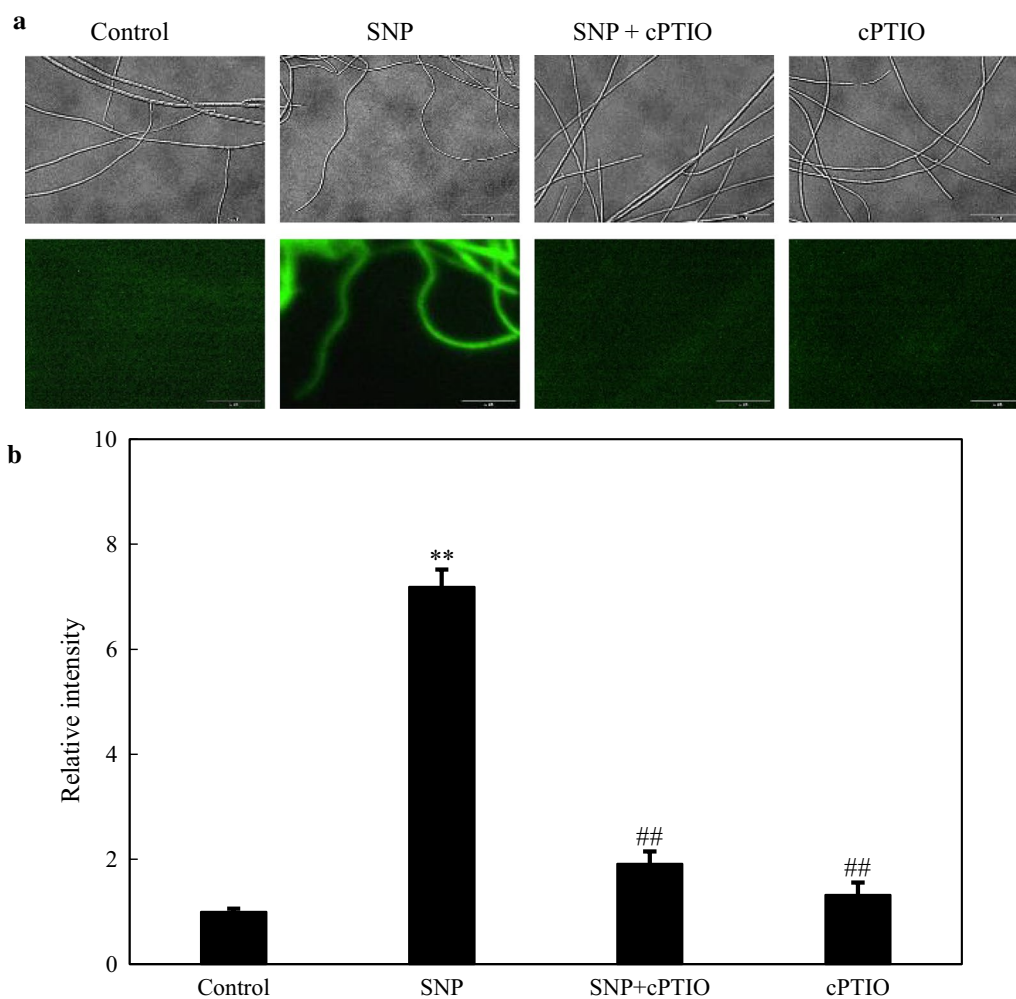


Fig. 1 NO generation in SNP-treated mycelia of *Shiraia* sp. S9. **a** Bright-field image (above) and fluorescence microscopy of DAF-2-DA-stained mycelium (below) in cultures. SNP was added at 0.10 mM on day 3 of the culture. cPTIO (0.10 mM) was added 30 min prior to SNP treatment. The photos were taken after 2 h of SNP treatment. **b** NO accumulation (relative intensity of fluorescent ratio) in mycelium after SNP treatment. Values are mean \pm SD from three independent experiments (** $p < 0.01$ vs. control, ## $p < 0.01$ vs. SNP group)

(Fig. 3c). The total HA production was enhanced to 110.34 mg/L on day 7, a 2.65-fold increase over the control without SNP addition (Fig. 3d).

SNP-induced transcriptional changes of genes for hypocrellin biosynthesis

To examine the transcriptional changes of *Shiraia* sp. S9 after SNP treatment, RNA-Seq experiment was subsequently performed. There were altogether 84,275 unigenes assembled with an average length of 1,011.81 bp (base pairs) and an N50 of 5,399 bp (Additional file 1: Table S1, Figure S6). 98.62%, 54.40%, 37.37%, 30.86% and 90.40% of the total unigenes were resemble to known genes reported in the current databases in Additional file 1: Table S2. A total of 571 differentially expressed

genes (DEGs) were identified (Additional file 2: Table S3), including up-regulated unigenes (355, 62.17%) and down-regulated unigenes (216, 37.83%) under SNP treatment (Additional file 1: Figure S7). These DEGs were categorized into the independent classification group “biological process (BP)”, “molecular function (MF)” and “cellular component (CC)” (Additional file 2: Table S4). Compared with the annotated unigenes of BP (270 DEGs) and CC (169 DEGs) (Additional file 1: Figure S8A, B), more than 322 DEGs were categorized into MF group (Additional file 1: Figure S8C). Within the MF category, DEGs (129 unigenes) assigned to ‘catalytic activity’ (GO:0003824) were of the highest proportion and other DEGs were mainly involved in ‘oxidoreductase activity’ (GO:0016491), ‘transporter activity’ (GO:0005215)

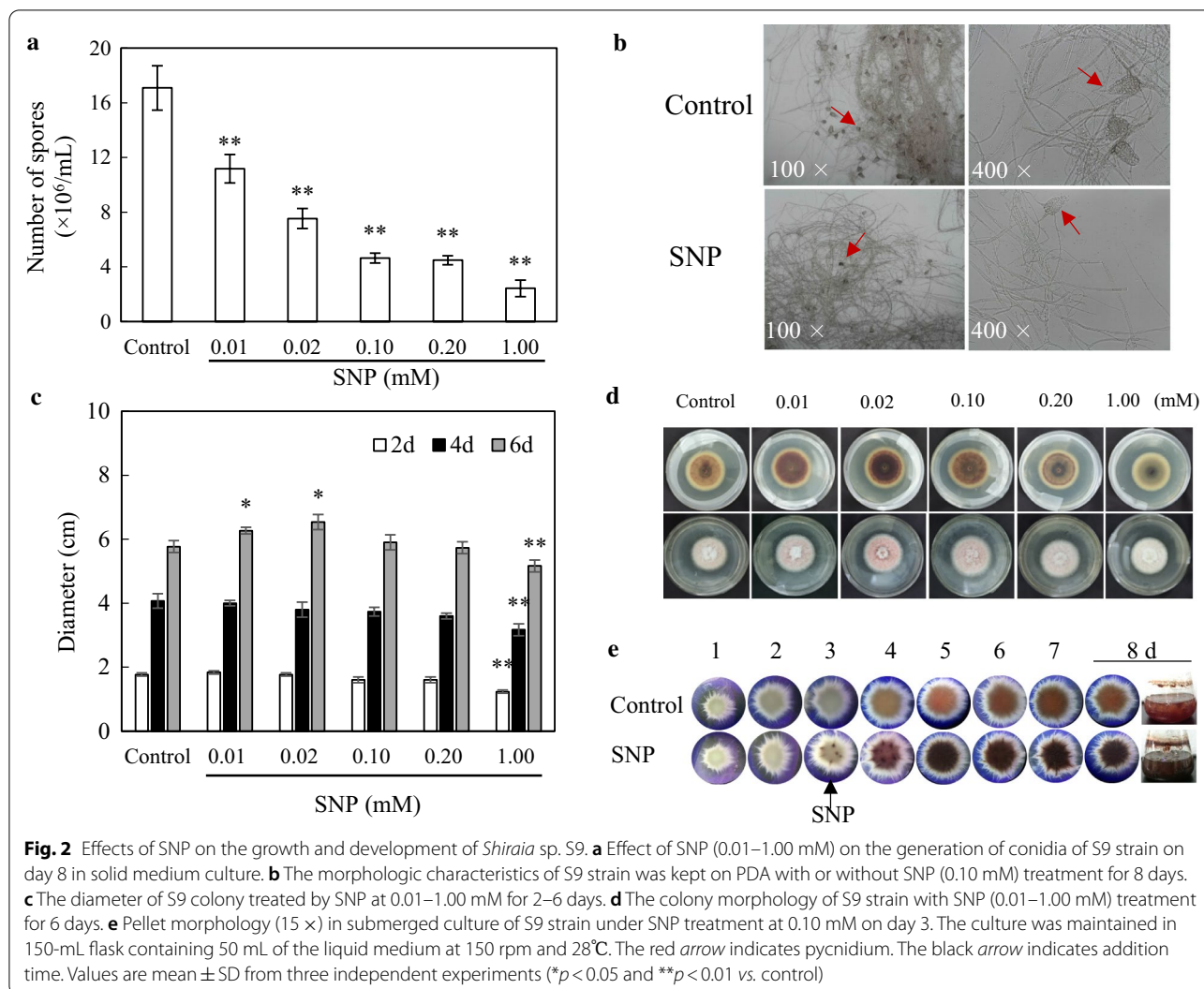


Table 1 Effects of SNP on the individual hypocrellin production in submerged cultures of *Shiraiia* sp. S9

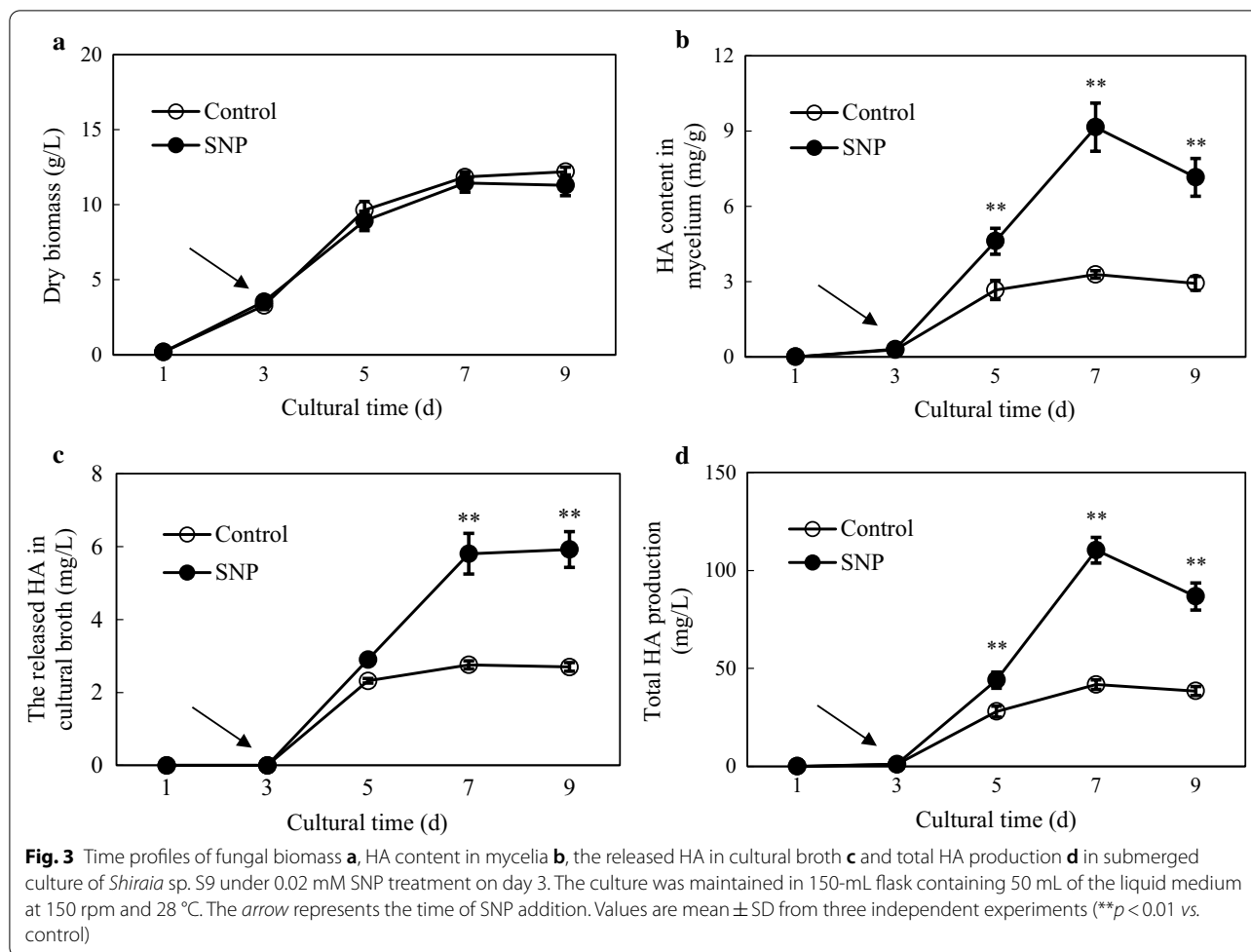
| PQ production (mg/L) | EC | EB | HC | EA | HA |
|-------------------------------------|-------------|-------------|-------------|----------------|---------------|
| Intracellular PQs in mycelia | | | | | |
| Control | 0.54 ± 0.05 | 1.03 ± 0.13 | 5.68 ± 1.90 | 1.93 ± 0.04 | 47.05 ± 3.30 |
| SNP | 0.50 ± 0.03 | 1.29 ± 0.23 | 7.38 ± 0.29 | 11.34 ± 0.78** | 57.54 ± 3.50* |
| Extracellular PQs in cultural broth | | | | | |
| Control | ND | ND | ND | 0.13 ± 0.04 | 2.25 ± 0.20 |
| SNP | ND | ND | ND | 0.14 ± 0.02 | 4.22 ± 0.40** |

The SNP at 0.10 mM was added into the mycelium cultures on day 3 and the culture was maintained in 150-mL flask containing 50 mL of the liquid medium at 150 rpm and 28 °C for 8 days. Values are mean ± SD from three independent experiments (**p* < 0.05 and ***p* < 0.01 vs. control). ND indicates no detection

and ‘transmembrane transporter activity’ (GO:0022857) items.

Based on the reported gene clusters for hypocrellin biosynthesis [27–29], we explored the expression changes of DEGs associated with hypocrellin

biosynthesis under SNP treatment. De novo sequencing and comparative analysis revealed 113 putative DEGs were enriched in 10 items related to fungal hypocrellin production (Additional file 2: Table S5 and S6), including ‘polyketide synthase’, ‘hydroxylase’,



‘probable metabolite transport protein,’ and so forth. Among them, more than 75% DEGs which are associated with intracellular hypocrellin biosynthesis were up-regulated compared with control group (Additional file 2: Table S5 and Fig. 4a), such as laccase-like multicopper oxidase (*MCO*, TRINITY_DN31904_c0_g1_i4), conidial yellow pigment biosynthesis polyketide synthase (*PKS*, TRINITY_DN73250_c0_g1_i1), hydroxyindole-*O*-methyltransferase (*OmeF*, TRINITY_DN28714_c0_g2_i1), FAD dependent oxidoreductase (*FAD*, TRINITY_DN33725_c0_g1_i8), phenol hydroxylase (*Hyd*, TRINITY_DN84020_c0_g1_i1), cytochrome P450 CYP2 subfamily (*Mono*, TRINITY_DN31508_c0_g2_i1), fasciclin (*Fas*, TRINITY_DN43991_c0_g1_i1) (Table 2). The expression levels of seven randomly selected unigenes related to hypocrellin biosynthesis were confirmed through qRT-PCR strictly (Fig. 4b), in which *Hyd* and *PKS* were more dramatically up-regulated by 59.35- and 14.59-fold, separately. The expression changes by qRT-PCR showed a similar tendency to those in transcriptome data (Table 2). In addition,

it was found that more than 60% DEGs bound up with extracellular HA exportation were also up-regulated (Additional file 2: Table S6), such as major facilitator superfamily (*MFS*, TRINITY_DN33647_c1_g1_i8), ABC superfamily (*ABC*, TRINITY_DN73211_c0_g2_i1), secondary metabolites biosynthesis, transport and catabolism (*MTP*, TRINITY_DN30127_c0_g1_i1) (Table 2). Meanwhile, the SNP-induced up-regulation of transcriptional expression of selected unigene *MFS* (TRINITY_DN33647_c1_g1_i8) from 2.40- to 7.31-fold was confirmed by qRT-PCR (Fig. 4c).

As shown in Additional file 2: Table S7, a total of 6440 unigenes were classified into 55 transcription factor (TF) groups, including C2H2, Trihelix, bZIP, bHLH, MYB related and so forth. Among all the TFs identified, bHLH (12.61%), ERF (7.47%), and MYB-related TF (7.08%) were of a higher proportion. Furthermore, there were altogether 189 DEGs enriched into 27 TFs differently expressed under SNP treatment (Additional file 2: Table S8), in which 24 TFs (110 DEGs) were up-regulated while 20 TFs (53 DEGs) were down-regulated

(See figure on next page.)

Fig. 4 a Heat map of DEGs involved in hypocrellin biosynthesis of *Shiraia* sp. S9 by SNP. **b** Validation of the expression levels of unigenes related to hypocrellin biosynthesis of S9 strain by qRT-PCR on day 8. *Hyd*, TRINITY_DN84020_c0_g1_i1. *PKS*, TRINITY_DN73347_c0_g1_i1. *MCO*, TRINITY_DN31904_c0_g1_i4. *FAD*, TRINITY_DN33725_c0_g1_i8. *Omef*, TRINITY_DN28714_c0_g2_i1. *Mono*, TRINITY_DN33456_c1_g1_i4. *Fas*, TRINITY_DN43991_c0_g1_i1. **c** Validation of the expression levels of *MFS* (TRINITY_DN33647_c1_g1_i8) by qRT-PCR. The SNP treatment was the same as specified in Fig. 3. Values are mean \pm SD from three independent experiments (** $p < 0.01$ vs. control)

in *Shiraia* mycelia. Among the up-regulated TFs, ERF ranked the highest (12 DEGs), followed by C3H (12 DEGs), and MYB (11 DEGs) (Table 2). Meanwhile, in the down-regulated TFs, NAC ranked the highest (8 DEGs), followed by C2H2 (6 DEGs), and bHLH (5 DEGs). Some prominent expression changes of unigenes associated with the high proportion of TFs were listed in Table 2, including several hypothetical proteins (TRINITY_DN31904_c0_g1_i4, TRINITY_DN33640_c0_g1_i50, TRINITY_DN33640_c0_g1_i25 and TRINITY_DN28413_c0_g1_i2), two aldehyde dehydrogenases (TRINITY_DN33276_c0_g1_i17 and TRINITY_DN33276_c0_g1_i28), hexose transporter-like protein (TRINITY_DN31580_c0_g1_i1), ATP binding (TRINITY_DN31301_c0_g1_i7).

SNP-induced transcriptional changes of genes involved in membrane permeabilization

On the basis of the analysis results from GO classification (Additional file 2: Table S4), a large number of unigenes were enriched into 'membrane' (61 DEGs of GO:0016020), 'transporter' (51 DEGs of GO:0006810), 'integral to membrane' (36 DEGs of GO:0016021), 'intrinsic to membrane' (36 DEGs of GO:0031224), 'membrane part' (36 DEGs of GO:0,044,425), 'transmembrane transport' (34 DEGs of GO:0055085), 'transporter activity' (33 DEGs of GO:0005215) and 'transmembrane transporter activity' (30 DEGs of GO:0022857) items after SNP application. Hence, we explored the alteration of hyphal cell membrane permeability and membrane lipid components of *Shiraia* sp. S9. As shown in Fig. 5, the fluorescence was strengthened in SYTOX Green-stained cells after SNP treatment, indicating the increased permeabilization of cell membrane. Simultaneously, we found that the composition proportions of some saturated fatty acids such as palmitic (C16:0) and stearic (C18:0) were decreased by 19.08% and 23.97%, respectively (Table 3). On the contrary, the proportions of four unsaturated fatty acids including palmitoleic (C16:1), oleic (C18:1), erucic (C22:1) and nervonic (C24:1) were raised significantly, up to 6.23-fold (Table 3). Hence, the ratio of unsaturated fatty acids with saturated ones was enhanced to 0.57 in the hyphal cells of S9 strain under SNP treatment, a 4.07-fold of the control group, suggesting the enhancement of cell membrane fluidity.

SNP-induced transcriptional changes of genes involved in oxidative stress

According to the transcriptome analysis, there were 121 DEGs enriched into 'oxidation-reduction process' (GO:0055114), 'oxidoreductase activity' (GO:0016491), 'electron carrier activity' (GO:0009055) and 'oxidoreductase activity, acting on paired donors, with incorporation or reduction of molecular oxygen' (GO:0016705) items (Additional file 2: Table S4), suggesting an oxidative stress induced by SNP. By comparison between control and SNP groups (Fig. 6a), the green fluorescent signals of 2, 7-dichlorodihydrofluorescein diacetate (DCFH-DA) in hyphal cells were brighter and more intense (4.72-fold, Fig. 6b), indicating the increase of ROS generation. When *Shiraia* sp. S9 was cultured in the presence of ROS scavenger vitamin C (Vc) and diphenyleneiodonium (DPI), an inhibitor of ROS generating enzyme NADPH oxidase (NOX) for 30 min prior to SNP application, the relative intensities of fluorescence in mycelia exhibited much more notable reduction of 72.39% and 72.14% (Fig. 6b) compared with the SNP group, separately. The content of superoxide anion (O_2^-) in mycelia was induced rapidly around 30 min of SNP treatment, reaching a highest value of 6.47 $\mu\text{mol/g}$ FW (fresh weight) with time up to day 7, which was 59.14% higher than that of control (Fig. 6c). The change trends of hydrogen peroxide (H_2O_2) concentration were consistent with O_2^- production. The generation of H_2O_2 was strikingly increased from 9.12 to 11.75 $\mu\text{mol/g}$ FW after 2–4-day treatment of SNP and then decreased on day 7–9, but it was still higher than those of the control group (Fig. 6d). As shown in Fig. 7, the activities and expression levels of three oxidoreductases were significantly stimulated by SNP. The most significant stimulation of enzyme activities of NOX, catalase (CAT) and superoxide dismutase (SOD) occurred on day 7, which were 157.71%, 85.49% and 64.71% higher than those of control, respectively. Accordingly, the transcriptional expression levels of NOX, CAT and SOD were activated on day 5 or 7, and the strongest induction effect appeared on day 7, about 3.71-, 2.90- and 4.21-fold of control, separately.

Discussion

SNP is a potent vasodilator used clinically to treat hypertensive emergencies and heart failure. In addition, it is widely used as nitric oxide donor in pharmacologic studies to investigate on the physiological roles of NO [14]. In plant cells or root cultures, SNP has been used as NO

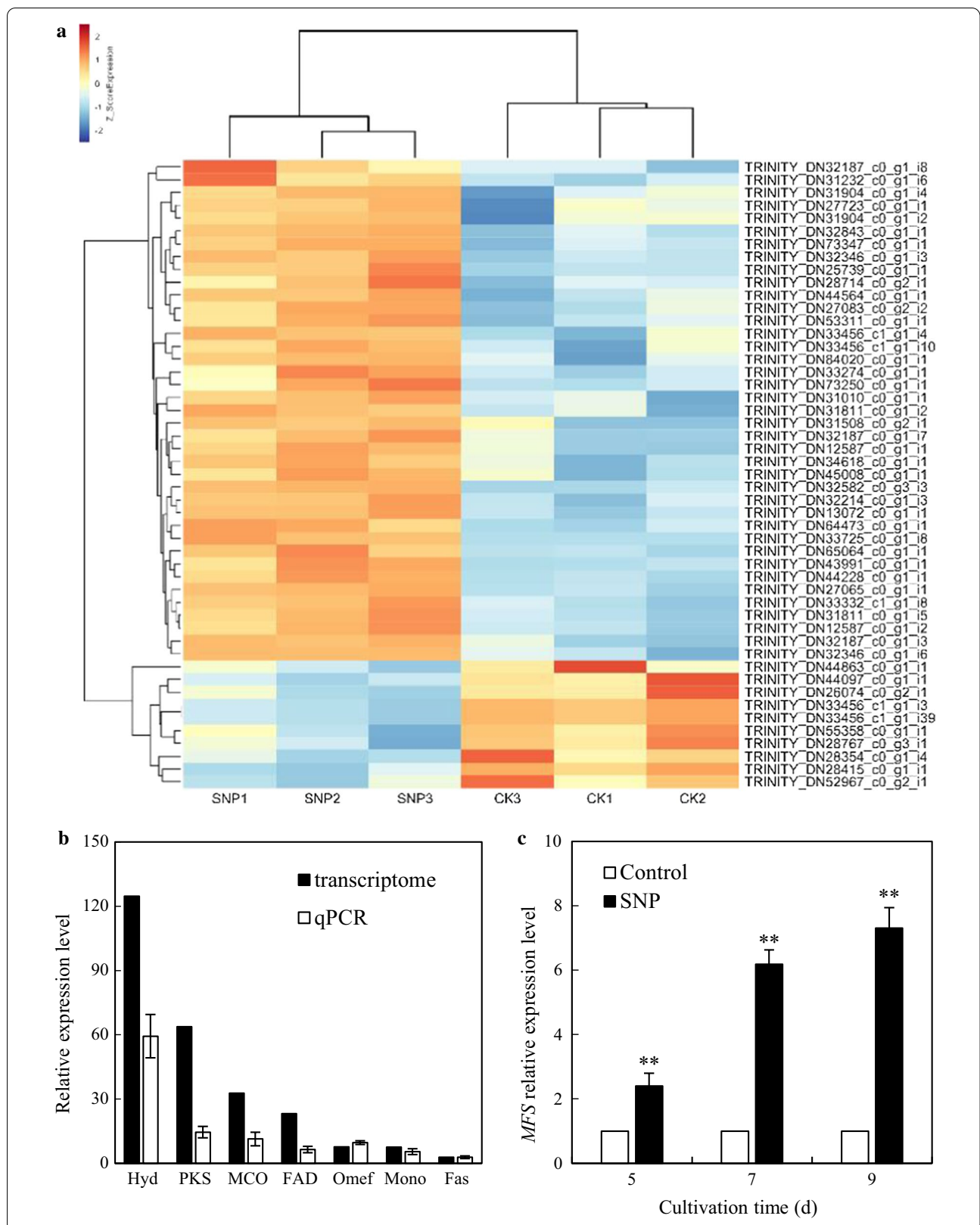


Table 2 Examples of DEGs involved in the hypocrellin biosynthesis, transport and transcription factors (TFs) of *Shiraia* sp. S9 by SNP

| Unigene ID | Up/down | Fold change ^a | Description |
|--|---------|--------------------------|--|
| Hypocrellin biosynthesis | | | |
| 1. Laccase-like multicopper oxidase (<i>MCO</i>) | | | |
| TRINITY_DN31904_c0_g1_i4 | Up | 32.8 | Multicopper oxidases [KOG1263] |
| TRINITY_DN31904_c0_g1_i2 | Up | 21.18 | Multicopper oxidases [KOG1263] |
| 2. Polyketide synthase (<i>PKS</i>) | | | |
| TRINITY_DN73347_c0_g1_i1 | Up | 63.84 | Iterative polyketide synthase CazM [A0A0K0MCJ4.1] |
| TRINITY_DN73250_c0_g1_i1 | Up | 7.18 | Conidial yellow pigment biosynthesis polyketide synthase [Q03149.2] |
| 3. O-methyltransferase (<i>OmeF</i>) | | | |
| TRINITY_DN28714_c0_g2_i1 | Up | 7.74 | Hydroxyindole-O-methyltransferase and related SAM-dependent methyltransferases [KOG3178] |
| TRINITY_DN32187_c0_g1_i3 | Up | 4.49 | Hydroxyindole-O-methyltransferase and related SAM-dependent methyltransferases [KOG3178] |
| 4. FAD/FMN-dependent oxidoreductase (<i>FAD</i>) | | | |
| TRINITY_DN33725_c0_g1_i8 | Up | 23.27 | FAD dependent oxidoreductase [OAL49443.1] |
| TRINITY_DN64473_c0_g1_i1 | Up | 4.7 | Uncharacterized FAD-linked oxidoreductase ARB_02478 [D4AS41.2] |
| 5. Hydroxylase (<i>Hyd</i>) | | | |
| TRINITY_DN84020_c0_g1_i1 | Up | 124.71 | Phenol hydroxylase [KMK58601.1] |
| TRINITY_DN13072_c0_g1_i1 | Up | 18.1 | Alkane hydroxylase 1 [Q9Y757.2] |
| 6. Monooxygenase (<i>Mono</i>) | | | |
| TRINITY_DN25739_c0_g1_i1 | Up | 20.83 | FAD-dependent monooxygenase andF [G3Y424.1] |
| TRINITY_DN31508_c0_g2_i1 | Up | 15.56 | Cytochrome P450 CYP2 subfamily [KOG0156] |
| 7. Fasciclin (<i>Fas</i>) | | | |
| TRINITY_DN43991_c0_g1_i1 | Up | 2.93 | Fasciclin and related adhesion glycoproteins [KOG1437] |
| Hypocrellin transport | | | |
| 1. Major facilitator superfamily (<i>MFS</i>) | | | |
| TRINITY_DN33647_c1_g1_i8 | Up | 43.12 | Major facilitator superfamily [KOG0255] |
| TRINITY_DN6606_c0_g1_i1 | Up | 37.62 | MFS quinate transporter-like protein QutD [OAL06848.1] |
| 2. ATP-binding cassette transporter (<i>ABC</i>) | | | |
| TRINITY_DN73211_c0_g2_i1 | Up | 2.60 | ABC superfamily [KOG0065] |
| TRINITY_DN30218_c0_g1_i2 | Down | 2.47 | ABC superfamily [KOG0055] |
| 3. Metabolite transport protein (<i>MTP</i>) | | | |
| TRINITY_DN30127_c0_g1_i1 | Up | 4.02 | Secondary metabolites biosynthesis, transport and catabolism [KOG0222] |
| TRINITY_DN25695_c4_g2_i1 | Up | 2.23 | Secondary metabolites biosynthesis, transport and catabolism [KOG1208] |
| Transcription factors (TFs) | | | |
| 1. ERF | | | |
| TRINITY_DN31904_c0_g1_i4 | Up | 5.04 | Hypothetical protein SNOG_06494 [XP_001796864.1] |
| TRINITY_DN31580_c0_g1_i1 | Up | 4.67 | Hexose transporter-like protein [OAK96729.1] |
| 2. C3H | | | |
| TRINITY_DN33456_c0_g1_i1 | Up | 2.36 | P-loop containing nucleoside triphosphate hydrolase protein [OAG15388.1] |
| TRINITY_DN31301_c0_g1_i7 | Up | 2.02 | ATP binding [KZM25621.1] |
| 3. MYB | | | |
| TRINITY_DN33687_c0_g1_i33 | Up | 7.01 | U4/U6-associated splicing factor PRP4 [KOG0670] |
| TRINITY_DN33611_c1_g2_i5 | Up | 6.67 | ATP-dependent RNA helicase MSS116 [OAL02684.1] |
| 4. NAC | | | |
| TRINITY_DN33640_c0_g1_i50 | Down | 8.87 | Hypothetical protein IQ06DRAFT_327513 [OAK97976.1] |
| TRINITY_DN33640_c0_g1_i25 | Down | 8.48 | Hypothetical protein SNOG_15601 [XP_001805746.1] |
| 5. C2H2 | | | |
| TRINITY_DN28764_c0_g1_i5 | Down | 2.74 | Acetyl-CoA synthetase-like protein [OAL06367.1] |
| TRINITY_DN28413_c0_g1_i2 | Down | 2.61 | Hypothetical protein SNOG_13514 [XP_001803722.1] |
| 6. bHLH | | | |
| TRINITY_DN33276_c0_g1_i17 | Down | 7.94 | Aldehyde dehydrogenase [OAK94834.1] |
| TRINITY_DN33276_c0_g1_i28 | Down | 6.32 | Aldehyde dehydrogenase [OAK94834.1] |

Table 2 (continued)

^a Fold change, up: ratio (S2/S1); down: ratio (S1/S2). S1, the FPKM value of the unigene in control group; S2, the FPKM value of the unigene in SNP group

Table 3 Effect of SNP treatment on fatty acid composition (% total fatty acid) of *Shiraia* sp. S9

| Fatty acid composition | Total fatty acid (%) | |
|--|----------------------|----------------|
| | Control | SNP |
| C16:0 | 24.21 ± 0.54 | 19.59 ± 1.07** |
| C18:0 | 15.02 ± 0.35 | 11.42 ± 0.16** |
| C23:0 | 0.18 ± 0.03 | 0.28 ± 0.05 |
| C16:1 | 3.49 ± 0.24 | 8.28 ± 0.21** |
| C18:1 | 1.17 ± 0.10 | 4.79 ± 0.42** |
| C22:1 | 0.62 ± 0.04 | 3.86 ± 0.57** |
| C24:1 | 0.29 ± 0.03 | 0.82 ± 0.11** |
| Unsaturated/saturated fatty acid ratio | 0.14 ± 0.01 | 0.57 ± 0.01** |

The SNP treatment was the same as specified in Fig. 3. Ratio of unsaturated/saturated fatty acid = (C16:1 + C18:1 + C22:1 + C24:1)/(C16:0 + C18:0 + C23:0). Values are mean ± SD from three independent experiments. ** $p < 0.01$ vs. control

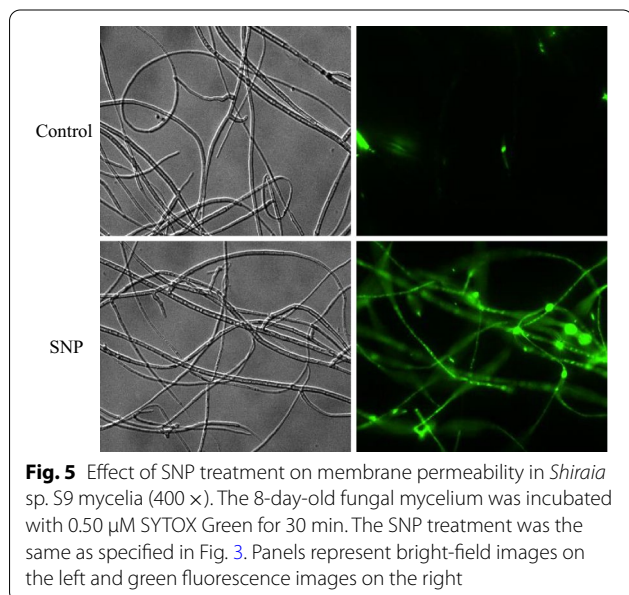
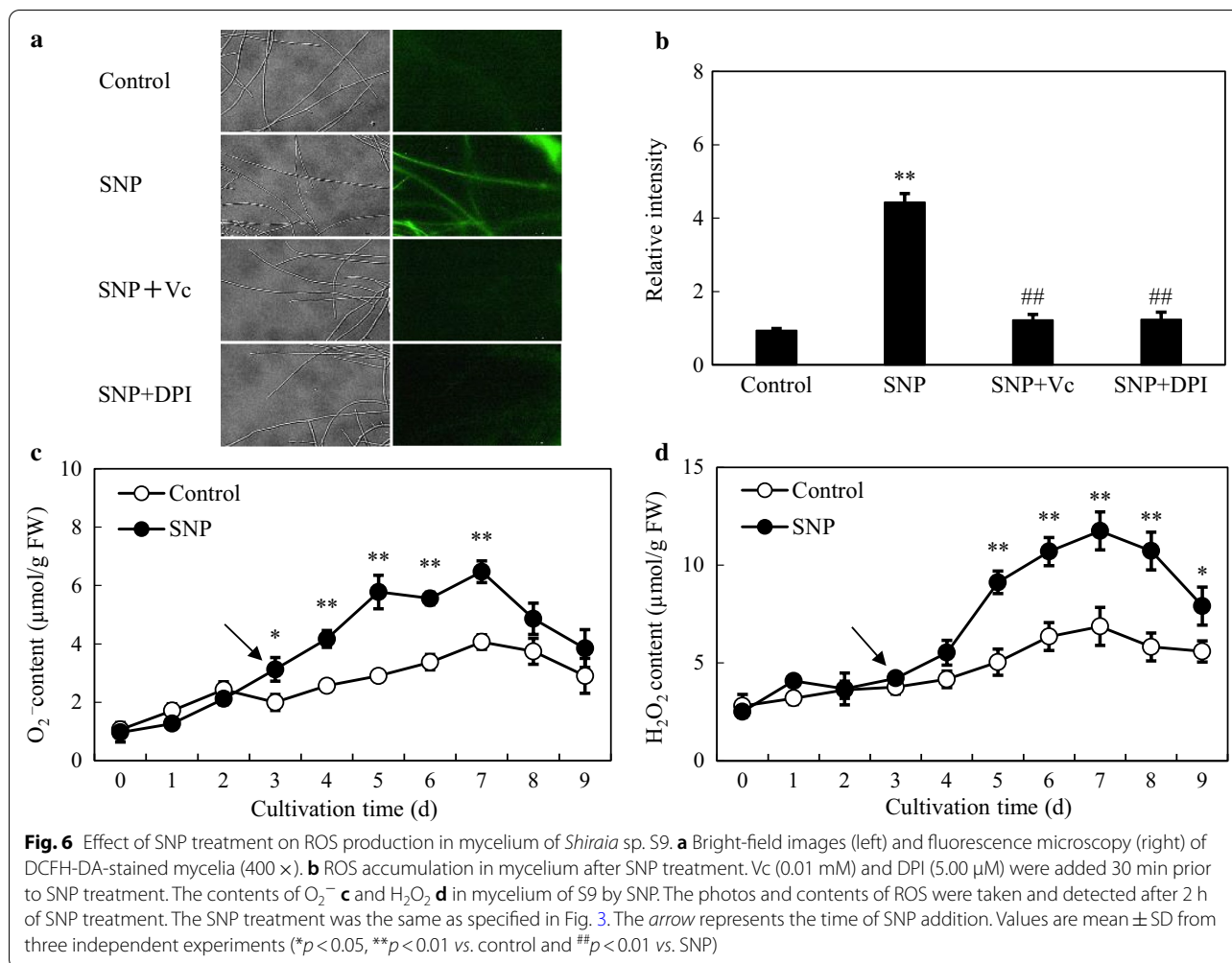


Fig. 5 Effect of SNP treatment on membrane permeability in *Shiraia* sp. S9 mycelia (400 ×). The 8-day-old fungal mycelium was incubated with 0.50 μM SYTOX Green for 30 min. The SNP treatment was the same as specified in Fig. 3. Panels represent bright-field images on the left and green fluorescence images on the right

donor to elicit the production of important bioactive secondary metabolites such as anthocyanin and flavonol glycoside in *Pisum sativum* [30], and tropane alkaloids in hair roots culture of *Hyoscyamus reticulatus* [31]. More recently, the signal roles of NO in fungal developmental and metabolic biosynthesis have drawn more attention [32]. With the help of using NO donor SNP and NO scavengers, previous studies indicated that NO modulated the germination of *C. coccodes* conidia [21], hyphal

elongation of *Magnaporthe oryzae* [33] and biosynthesis of fungal secondary metabolites such as styrylpyrone polyphenols, flavonoids and phenolics [23, 34]. However, it is less reported on SNP application as a chemical elicitor to enhance fungal metabolite production in mycelium cultures. In submerged cultures of *G. lucidum*, the eliciting effects of SNP at 0.5–5.0 mM on ganoderic triterpenoid production were investigated over 120 h [24]. The yields of ganoderic triterpenoids were increased by 40.94% at 72 h after SNP treatment at 5 mM. In our present study, NO elicited the biosynthesis of hypocrellins in *Shiraia* sp. S9, especially increased EA and HA contents in the mycelia (Table 1 and Additional file 1: Figure S3). After the optimization of the conditions for SNP application (the concentration and adding time) (Additional file 1: Figure S4 and S5), a higher production of HA (110.34 mg/L) was induced by SNP at 0.02 mM on day 7, a 2.65-fold increase over the control (Fig. 3). Compared with other elicitors used to promote HA production in *Shiraia* cultures including light irradiation [35, 36], ultrasound exposure [25] or microbial elicitors [9, 37], the chemical elicitor SNP has the advantages of lower cost, easy preparation, no growth suppression, and high efficiency for eliciting metabolite production in the mycelium cultures.

In our study, a rapid generation of endogenous NO was observed when SNP was applied (Fig. 1). The generated NO in mycelia was fully suppressed by a NO scavenger cPTIO, indicating exogenous SNP as a NO producer in the culture. Accumulating evidence showed NO could collaborate with the accompanied generation of ROS to form nitro-oxidative stress involved in human or plant diseases [14, 38]. Zheng et al. (2010) reported that the SNP (50 μM) promoted the H₂O₂ content in the hairy roots of *A. annua* elicited by fungal oligosaccharides [39]. SNP at 250 μM could enhance H₂O₂ level in adventitious roots of *E. purpurea* [17]. In this study, SNP treatment also resulted in an accumulation of ROS including O₂⁻ and H₂O₂ in the mycelia (Fig. 6). Simultaneously, GO analysis demonstrated the enriched DEGs of ‘oxidation–reduction process’ (GO:0055114), ‘oxidoreductase activity’ (GO:0016491) and ‘electron carrier activity’ (GO:0009055) in the group of molecular function (Additional file 1: Figure S8 and Additional file 2: Table S4). Both the gene expressions of ROS generating NOX and the activities of antioxidant enzymes such as CAT and SOD were validated in SNP-treated mycelia (Fig. 7), suggesting that SNP could activate NOX for the increased oxidative stress in the mycelium cultures. In fungal



cultures, ROS could provoke the production of fungal secondary metabolites, such as carotenoid in *Neurospora crassa* [40], deoxynivalenol in *Fusarium graminearum* [41], ochratoxin A in *A. ochraceus* [42]. In our previous researches, ROS generation and oxidative stress were reported as early signal-response events leading to HA biosynthesis of *Shiraia* under various abiotic elicitors, including the applications of surfactant Triton X-100 [10], lower intensity ultrasound [25] and light–dark shift [35]. These studies indicated the oxidative stress was involved in the hypocrellin biosynthesis of *Shiraia*. In our present study, we found 54 putative unigenes from 571 DEGs probably involved in hypocrellin biosynthesis after SNP treatment (Additional file 2: Table S5 and Fig. 4a). It was supposed that hypocrellins were biosynthesized in fungal cells via repetitive decarboxylative condensation of acetyl- and malonyl-CoA by polyketide synthase (*PKS*), methylation, decarboxylation and reduction by *O*-methyltransferase (*Omef*), monooxygenase/hydroxylase (*Mono/Hyd*) and multicopper oxidase (*MCO*), and

then the core structure formation via the cooperation of fasciclin (*Fas*), laccase and berberine bridge enzyme (*BBE*) [28, 43, 44]. The deletion and overexpression of *SbaPKS* indicated its essential role in the hypocrellin biosynthesis of *Shiraia* sp. SUPER-H168 [45]. *SbaPKS* also had a moderating effect on the transcriptional expression of its adjacent genes *FAD*, *Omef*, *Mono* and *MCO* in the gene cluster. Overexpression of *Hyd* gene in *S. bambusicola* S4201 resulted in ultra-higher production of HA (1180.1 mg/L) [46]. Most of above-mentioned unigenes have been up-regulated significantly in our present experiment after SNP application, especially the expression of *Hyd* (59.35-fold) and *PKS* (14.59-fold) genes (Fig. 4b). The first transcription factor involved in HA biosynthesis is the zinc finger transcription factor *zftf* [29]. The *zftf* gene with a GAL4-like Zn(II)₂Cys₆ (or C6 zinc) binuclear cluster DNA-binding domain is located in the hypocrellin gene cluster. However, *zftf* is not the differentially expressed gene induced by SNP treatment (Additional file 2: Table S8). The up-regulated TFs were

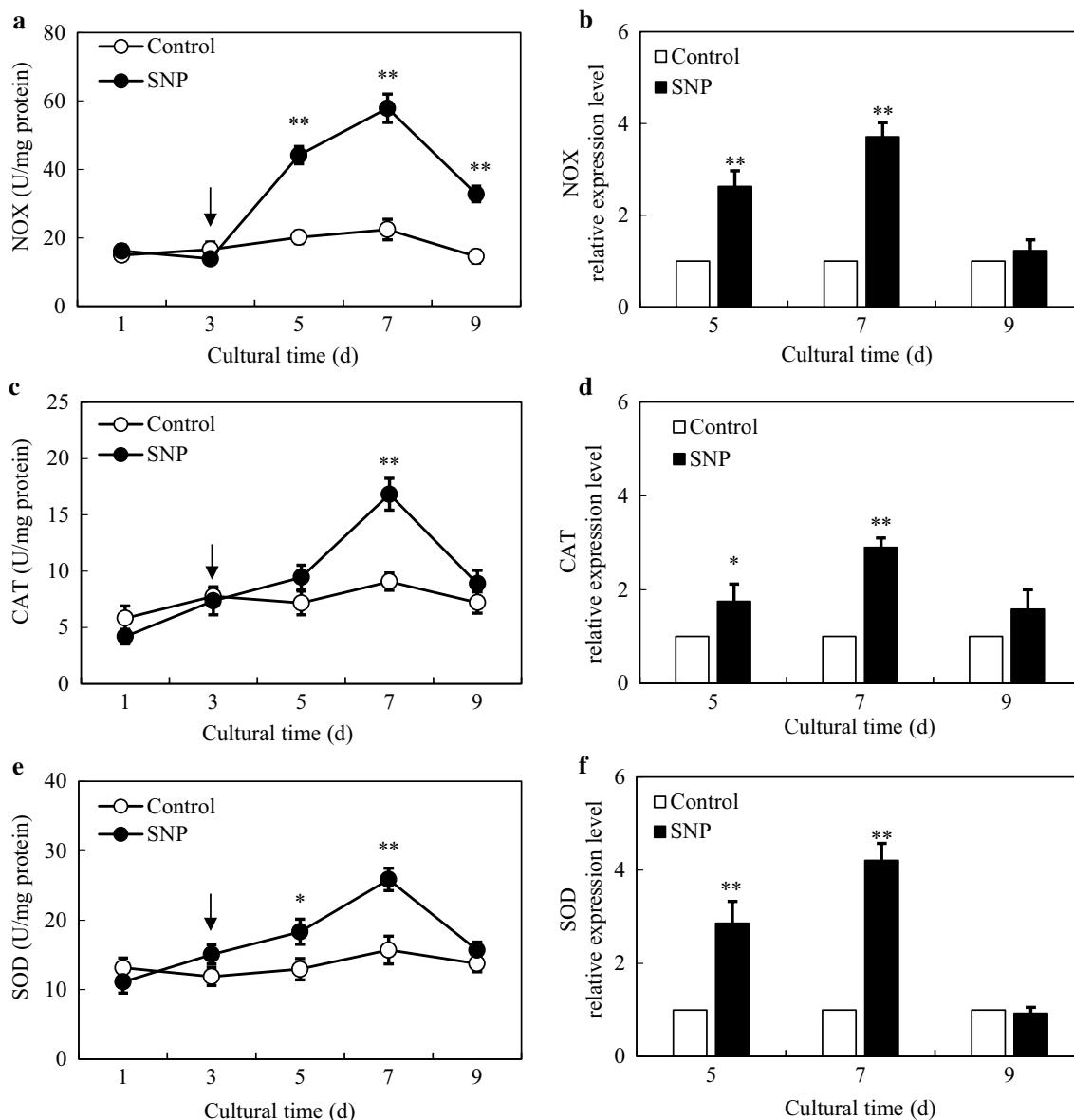


Fig. 7 Effects of SNP treatment on activities and expressions of *NOX* (a, b), *CAT* (c, d) and *SOD* (e, f) in *Shiraia* sp. S9 mycelium on day 1–9. *NOX* (comp2367_c0_seq1), *CAT* (comp15524_c0_seq1), *SOD* (CL8477Contig1). The SNP treatment was the same as specified in Fig. 3. The arrow represents the time of SNP addition. Values are mean \pm SD from three independent experiments (* $p < 0.05$ and ** $p < 0.01$ vs. control)

detected in the present study, including ERF, C3H and MYB (Table 2). These TFs have been studied extensively in initiating plant stress responses through involvement in the biosynthesis of secondary metabolites such as terpenoid indole alkaloids, taxol, flavonoids and proanthocyanins [47]. The challenge would be to elucidate the regulatory role of these TFs in regulation of HA biosynthesis. Taken together, the results from our present study have shown that SNP induced oxidative stress and activated genes and TFs for hypocrellin biosynthesis. The

relationship between NO and ROS, and the mechanism of their mediation on hypocrellin biosynthesis are being further investigated.

It is worth noting that SNP could promote hypocrellin both inside the hyphae and from the medium (Fig. 3). In mycelium cultures after SNP application, the released HA in culture medium was increased by 26.09–119.26% (Fig. 3c). Although the increased extracellular HA accounts for only 5.26–6.83% of total HA production, the results still implicated the efflux

of hypocrellins induced by SNP. Our GO classification revealed that the enriched DEGs were mainly in the categories of ‘membrane’ (GO:0016020), ‘integral to membrane’ (GO:0016021), ‘transmembrane transport’ (GO:0055085) and ‘transporter activity’ after SNP application (Additional file 1: Figure S8 and Additional file 2: Table S4). SNP treatment increased the proportion of total unsaturated fatty acids in the membranes of fungal hyphae (Table 3), leading to the enhanced membrane permeability (Fig. 5). On the other hand, membrane transporters have been reported to convey a photoactivated toxin cercosporin from *Cercospora* fungi for the auto-resistance [48]. Our RNA-Seq data also displayed that 32 unigenes encoding the transporter protein major facilitator superfamily (*MFS*) were up-regulated significantly (Additional file 2: Table S6). The qRT-PCR results also validated that the increases of gene expression levels of *MFS* (unigenes No. TRINITY_DN33647_c1_g1_i8) (2.40- to 7.31-folds) after SNP application (Fig. 4b). These results indicated that SNP could induce changes of membrane permeability and activate membrane transporter such as *MFS* to facilitate the secretion of hypocrellins.

Conclusion

Although endogenous NO generation was investigated in *Shiraia* mycelium cultures under the treatment of fungal elicitors [8, 12], the regulation on fungal metabolites by NO has not been well studied. To the best of our knowledge, it is the first time to use SNP as a chemical elicitor in mycelium cultures to promote hypocrellin productions. SNP at a higher concentration (0.02 mM) acted as a pro-oxidant, thereby raising the ROS generation, up-regulating biosynthetic genes for hypocrellin production. The increased membrane permeability and gene expression of member transporters induced by SNP was associated with efflux of hypocrellins. Our results showed the increase of total hypocrellin production is mainly attributed to the cellular hypocrellin biosynthesis and the efflux. When the mycelium cultures were treated by SNP at 0.02 mM for 4 days, the highest production (110.34 mg/L) of HA was achieved without any fungal growth depression. Although the mechanism of the SNP elicitation needs further investigation, the present study successfully provided a novel chemical elicitor for the biotechnological production of hypocrellins. This study is useful for hypocrellin production in a large-scale culture of *Shiraia* and facilitates the exploring of unknown genes and novel fungal secondary metabolites induced by SNP.

Materials and methods

Strain, media and culture conditions

The strain *Shiraia* sp. S9 (CGMCC16369) for hypocrellin production was obtained from fresh *Shiraia* fruit-body in our previous work [49]. The strain was maintained and stored at 4 °C on a potato dextrose agar (PDA) slant and initially grown at 28 °C for 8 days. The details of medium components and culture conditions were provided by our previous report [25]. The seed broth (2 mL) of S9 was transferred into a 150-mL Erlenmeyer flask containing 50-mL liquid medium and maintained in a rotary shaker at 150 rpm for 9 days at 28 °C.

SNP application

SNP (Beyotime Biotechnology, Jiangsu, China) was dissolved in deionized water at 0.50 mM as a stock solution and filtered through a sieve (Ø0.22 µm) before use. To determine the optimal dosage of SNP for hypocrellin production, different dosages (0.01–1.00 mM) of SNP were added into the cultural broth on day 3. To confirm the effect of the addition time, 0.02 mM SNP was added into the mycelium culture on day 1–5 respectively.

Measurement of medium pH, residual glucose and NO accumulation

The medium pH of the cultural broth was detected with pH Meter (FE20, Mettler Toledo, Zurich), and the residual glucose in cultural broth was measured using anthrone-sulfuric acid method [50]. To detect the NO accumulation in *Shiraia* sp. S9 mycelia, the NO-specific fluorescent probe DAF-2-DA (Sigma-Aldrich, St. Louis, MO, USA) was applied [51]. After 3 days of initial culture, DAF-2-DA (0.50 µM) was added to the cultural broth prior to SNP (0.10 mM) treatment. The NO scavenger cPTIO at 0.10 mM was added 30 min prior to SNP treatment [13]. After 2 h of incubation, a fluorescent microscope (Olympus Cell'R IX81, Center Valley, PA, USA) with excitation/emission wavelengths (470 nm/525 nm) was used for fluorescence observation.

Observation of morphological characteristics

To analyze the effect of SNP (0.01–1.00 mM) on growth and morphological changes of *Shiraia* sp. S9 during the solid medium culture, the colony diameter was measured in triplicates (3 objects in a replicate). Photos were taken on day 6. To investigate the influence of SNP on fungal development, the 8-day-old colony was eluted with 10-mL deionized water. Subsequently, the fungal morphological characteristics were observed and photographed by a light microscope (CKX41, Olympus, Tokyo, Japan). To observe the influence of SNP on fungal growth during the submerged culture, SNP at 0.10 mM was added into the cultural broth on day 3. The mycelia were

harvested and dried to constant weight at 60 °C to assess fungal biomass. The fungal pellets were viewed and photographed under a stereoscopic microscope (SMZ1000, Nikon, Tokyo, Japan). Pellet diameters were measured in triplicates (50 pellets per replicate).

Analysis of cell membrane permeability

The membrane permeabilization of hyphal cell was detected by SYTOX Green dye, a high-affinity nucleic acid stain fluorescent probe (Eugene, Oregon, USA) [52]. After 5 days of the initial culture of S9 strain, the harvested hyphae were incubated with the fluorescent probe solution (0.50 μ M) for 30 min, and then the fluorescence intensity was observed and analyzed by means of an Olympus fluorescent microscope (CKX41, Tokyo, Japan) with the excitation/emission wavelengths at 488/538 nm respectively.

The components of mycelial fatty acids were extracted and analyzed via the protocols given in our previous report [10]. The detection of fungal fatty acids was carried out by using a gas chromatograph (Agilent7820, Palo Alto, CA, USA) with an Agilent DB-23 column (30.00 m \times 0.25 mm dimension). The fatty acids were quantified with their internal standards purchased from Sigma-Aldrich (St. Louis, MO, USA).

Measurement of ROS accumulation and activities of antioxidant enzymes

The ROS generation in hyphal cell was detected by DCFH-DA (Beyotime Biotechnology, Haimen, China) probe, which could penetrate the cell membrane freely [53]. After 2 h of SNP treatment, the harvested hyphae were incubated with the fluorescent dye solution (0.01 mM) for 1 h, and then the fluorescence intensity was observed and photographed by means of an Olympus fluorescent microscope (CKX41, Tokyo, Japan) with the excitation/emission wavelengths at 485/528 nm. The relative fluorescence value is defined to the ratio of fluorescence intensity at 'SNP' group to that at 'Control' group. Simultaneously, the contents of H₂O₂ and O₂⁻ in the mycelia were assayed as previously described [54, 55]. The activities of NOX, CAT and SOD were measured using Enzyme Activity Assay Kit (Beyotime Biotechnology, Nanjing, China) according to the manufacturer's protocol and previous reports [56–58].

To study the effects of ROS signal during the culture of S9 strain by SNP, Vc and DPI were used as ROS scavenger and NOX inhibitor, respectively. The concentrations of ROS scavenger and NOX inhibitor used in this work were chosen based on previous research [59]. Vc (0.01 mM) and DPI (5.00 μ M) were added to the culture at 30 min prior to the application of SNP (0.02 mM) on day 3. The relative fluorescence value is defined to the ratio

of fluorescence intensity at 'SNP + Vc' or 'SNP + DPI' groups to that at 'SNP' group.

Detection of hypocrellin production

To analyze the influence of SNP on hypocrellin production in *Shiraia* sp. S9, SNP at 0.10 mM was added on day 3 and cultivated for 8 days. The hypocrellins in fungal mycelium and cultural broth were extracted based on the previous report [60]. The individual hypocrellin was quantified using a reverse-phase Agilent 1260 HPLC system (Agilent Co., Wilmington, USA) equipped with 250.0 mm \times 4.6 mm Agilent HC-C18 column. Samples were eluted with a mobile phase of acetonitrile: water (65: 35, v/v) at 1 mL/min for 20 min and monitored at 465 nm. Individual hypocrellin was quantified separately with genuine standards provided by the Chinese National Compound Library (CNCL, Shanghai, China). Total hypocrellin production refers to the sum of intracellular and extracellular hypocrellin.

Transcriptome sequencing, annotation and analysis

In this study, six samples with or without SNP treatment were obtained from three biological replicates (independent experiments) to establish cDNA libraries. Then, the HiSeq X Ten platform (Illumina, San Diego, CA, USA) was applied to sequence above cDNA libraries. The raw reads were cleaned and assembled according to our previous report [61]. All unigenes were subsequently annotated based on Basic Local Alignment Search Tool (BLAST) searches (version 2.2.31+) against Gene Ontology (GO, <http://www.geneontology.org/>) database with a cut off *E* value of $\leq 1e^{-5}$. The raw RNA-seq data have been submitted to NCBI's Gene Expression Omnibus (GEO) repository under accession number SRR7293200-7293205. In our study, we calculated the relative expression levels of genes via the fragments per kilobase per million reads (FPKM) method described by Mortazavi et al. [62]. Meanwhile, the significance of gene expression differences was evaluated using the cut-off criteria of $|\text{foldchange}| \geq 2$ and *p* value < 0.05 .

Quantitative real-time polymerase chain reaction (qRT-PCR)

Total RNA was extracted using RNAprep pure Plant Kit (Tiangen, Beijing, China) according to the instruction. The primer sequences of 18S ribosomal RNA (internal reference gene) and selected unigenes from NCBI database of SRR7293200-7,293,205 and PRJNA323638 were listed in Additional file 1: Table S9. The qRT-PCR was performed according to the method in our previous study [61]. And, the transcriptional expression levels of selected genes were calculated from cycle threshold

values by using the $2^{-\Delta\Delta CT}$ method described in detail by Zhang et al. [63].

Statistical analysis

Data analyses were carried out using Microsoft Excel and expressed as Mean \pm Standard Deviation (SD). Student's *t*-test was applied for the comparison of the means between two groups. One-way analysis of variance (ANOVA) test was used for the comparison of the means among multiple groups. $p < 0.05$ is considered statistically significant.

Supplementary Information

The online version contains supplementary material available at <https://doi.org/10.1186/s12934-021-01581-8>.

Additional file 1: Table S1. Illumina RNA-Seq reads and de novo assembly statistics of *Shiraia* sp. S9 by SNP. **Table S2.** Summary statistics of unigene annotation numbers of *Shiraia* sp. S9 by SNP. **Table S9.** Primers and relevant information of reference and target genes. F: forward primer, R: reverse primer. **Figure S1.** Effect of SNP at 0.10 mM on the growth and development of *Shiraia* sp. S9 in submerged culture. Time profiles of fungal biomass (A) and average pellet diameters (B) during the production culture. **Figure S2.** Time profiles of pH (A) and residual sugar (B) in *Shiraia* sp. S9 submerged cultures with the addition of SNP at 0.10 mM. **Figure S3.** Chromatograms of PQs in mycelium of *Shiraia* sp. S9 treated by SNP (0.10 mM) on day 3 and cultivated for 8 days. **Figure S4.** Effect of SNP concentration on (A) hyphal growth, (B) HA content in mycelium and (C) the released HA in cultural broth of *Shiraia* sp. S9. The strain was treated by SNP (0.01–1.00 mM) on day 3. **Figure S5.** Effect of SNP addition time on (A) hyphal growth, (B) HA content in mycelium and (C) the released HA in cultural broth of *Shiraia* sp. S9. SNP (0.02 mM) was added on different cultural time (1–5 d). **Figure S6.** The length distribution of unigenes of *Shiraia* sp. S9 by SNP. **Figure S7.** Heat map of DEGs summary of *Shiraia* sp. S9 by SNP. The up/down-regulated DEGs were detected by comparing RNA-Seq data of the unigenes of case group to control group (up: ratio > 1, down: ratio < 1). **Figure S8.** The cellular component (CC), biological process (BP) and molecular function (MF) of gene ontology (GO) categories of the DEGs in *Shiraia* sp. S9 under SNP treatment at 0.02 mM. The arrow represents the time of SNP addition. Values are mean \pm SD from three independent experiments (** $p < 0.01$ vs. control). Different letters above the bars mean significant differences ($p < 0.05$).

Additional file 2: Table S3. Annotation of DEGs using NR, SWISS-Prot, KEGG, KOG and GO databases and their fold change with SNP treatment. **Table S4.** GO enrichment of *Shiraia* sp. S9 with SNP treatment. **Table S5.** Differentially expressed genes (DEGs) involved in hypocrellin biosynthesis of *Shiraia* sp. S9 under SNP treatment. **Table S6.** Differentially expressed genes (DEGs) involved in hypocrellin transport of *Shiraia* sp. S9 under SNP treatment. **Table S7.** Annotation of transcription factors in *Shiraia* sp. S9. **Table S8.** Differentially expressed genes (DEGs) involved in transcription factors of *Shiraia* sp. S9 under SNP treatment.

Acknowledgements

Not applicable.

Authors' contributions

JWW and YJM conceived the study and participated in its design. YW, XPL and YJM undertook experiments and data analysis. YJM, XPL and YW drafted the manuscript. JWW supervised the research and revised the paper. All authors read and approved the final manuscript.

Funding

This work was supported by the National Natural Science Foundation of China (Nos. 82073955 and 81773696) and the Priority Academic Program Development of the Jiangsu Higher Education Institutes (PAPD).

Availability of data and materials

All data generated or analyzed during this study are included in this published article and its Additional files.

Declarations

Ethics approval and consent to participate

Not applicable.

Consent for publication

Not applicable.

Competing interests

The authors declare that they have no competing interests.

Author details

¹College of Pharmaceutical Sciences, Soochow University, Suzhou 215123, China. ²College of Life Sciences, Northwest Normal University, Lanzhou 730000, China.

Received: 15 December 2020 Accepted: 17 April 2021

Published online: 28 April 2021

References

- Zhen J, Di W. Novel therapeutic and diagnostic applications of hypocrellins and hypericins. *Photochem Photobiol.* 1995;61:529–39.
- Dai DQ, Phookamsak R, Wijayawardene NN, Li WJ, Bhat DJ, Xu JC, et al. Bambusicolous fungi. *Fungal Divers.* 2017;82:1–105.
- Kishi T, Tahara S, Taniguchi N, Tsuda M, Tanaka C, Takahashi S. New perylenequinones from *Shiraia bambusicola*. *Planta Med.* 1991;57:376–9.
- Mulrooney CA, O'Brien EM, Morgan BJ, Kozlowski MC. Perylenequinones: isolation, synthesis, and biological activity. *Eur J Org Chem.* 2012;21:3887–904.
- O'Brien EM, Morgan BJ, Mulrooney CA, Carroll PJ, Kozlowski MC. Perylenequinone natural products: total synthesis of hypocrellin A. *J Org Chem.* 2010;75:57–68.
- Cai YJ, Liang XH, Liao XR, Ding YR, Sun J, Li XH. High-yield hypocrellin A production in solid-state fermentation by *Shiraia* sp. SUPER-H168. *Appl Biochem Biotechnol.* 2010;160:2275–86.
- Yang HL, Xiao C, Ma W, He G. The production of hypocrellin colorants by submerged cultivation of the medicinal fungus *Shiraia bambusicola*. *Dyes Pigm.* 2009;82:142–6.
- Du W, Sun CL, Wang BG, Wang YM, Dong B, Liu JH, et al. Response mechanism of hypocrellin colorants biosynthesis by *Shiraia bambusicola* to elicitor PB90. *AMB Expr.* 2019;9:146.
- Ma YJ, Zheng LP, Wang JW. Inducing perylenequinone production from a bambusicolous fungus *Shiraia* sp. S9 through co-culture with a fruiting body-associated bacterium *Pseudomonas fulva* SB1. *Microb Cell Fact.* 2019;18:121.
- Lei XY, Zhang MY, Ma YJ, Wang JW. Transcriptomic responses involved in enhanced production of hypocrellin A by addition of Triton X-100 in submerged cultures of *Shiraia bambusicola*. *J Ind Microbiol Biotechnol.* 2017;44:1415–29.
- Li XP, Ma YJ, Wang JW. Adding bamboo charcoal powder to *Shiraia bambusicola* preculture improves hypocrellin A production. *Sustain Chem Pharm.* 2019;14:100191.
- Du W, Liang JD, Han YF, Yu JP, Liang ZQ. Nitric oxide mediates hypocrellin accumulation induced by fungal elicitor in submerged cultures of *Shiraia bambusicola*. *Biotechnol Lett.* 2015;37:153–9.
- Li XP, Wang Y, Ma YJ, Wang JW, Zheng LP. Nitric oxide and hydrogen peroxide signaling in extractive *Shiraia* fermentation by Triton X-100 for hypocrellin A production. *Int J Mol Sci.* 2020;21:882.

14. Tuteja N, Chandra M, Tuteja R, Misra MK. Nitric oxide as a unique bioactive signaling messenger in physiology and pathophysiology. *J Biomed Biotechnol*. 2004;4:227–37.
15. Zhang B, Zheng LP, Wang JW. Nitric oxide elicitation for secondary metabolite production in cultured plant cells. *Appl Microbiol Biotechnol*. 2012;93:455–66.
16. Farouk S, Al-Huqail AA. Sodium nitroprusside application regulates antioxidant capacity, improves phytopharmaceutical production and essential oil yield of marjoram herb under drought. *Ind Crops Prod*. 2020;158:113034.
17. Wu CH, Tewari RK, Hahn EJ, Paek KY. Nitric oxide elicitation induces the accumulation of secondary metabolites and antioxidant defense in adventitious roots of *Echinacea purpurea*. *J Plant Biol*. 2007;50:636–43.
18. Zheng LP, Guo YT, Wang JW, Tan RX. Nitric oxide potentiates oligosaccharide-induced artemisinin production in *Artemisia annua* hairy roots. *J Integr Plant Biol*. 2008;50:49–55.
19. Wang JW, Zheng LP, Wu JY, Tan RX. Involvement of nitric oxide in oxidative burst, phenylalanine ammonia-lyase activation and taxol production induced by low-energy ultrasound in *Taxus yunnanensis* cell suspension cultures. *Nitric Oxide*. 2006;15:351–8.
20. Gong XY, Fu YP, Jiang DH, Li GQ, Yi XH, Peng YL. L-Arginine is essential for conidiation in the filamentous fungus *Coniothyrium minitans*. *Fungal Genet Biol*. 2007;44:1368–79.
21. Wang J, Higgins VJ. Nitric oxide has a regulatory effect in the germination of conidia of *Colletotrichum coccodes*. *Fungal Genet Biol*. 2005;42:284–92.
22. Baidya S, Cary JW, Grayburn WS, Calvo AM. Role of nitric oxide and flavohemoglobin homolog genes in *Aspergillus nidulans* sexual development and mycotoxin production. *Appl Environ Microbiol*. 2011;77:5524–8.
23. Zhao YX, Xi Q, Xu Q, He MH, Ding JN, Dai YC, et al. Correlation of nitric oxide produced by an inducible nitric oxide synthase-like protein with enhanced expression of the phenylpropanoid pathway in *Inonotus obliquus* cocultured with *Phellinus morii*. *Appl Microbiol Biotechnol*. 2015;99:4361–72.
24. Gu L, Zhong X, Lian DH, Zheng YM, Wang HZ, Liu X. Triterpenoid biosynthesis and the transcriptional response elicited by nitric oxide in submerged fermenting *Ganoderma lucidum*. *Process Biochem*. 2017;60:19–26.
25. Sun CX, Ma YJ, Wang JW. Enhanced production of hypocrellin A by ultrasound stimulation in submerged cultures of *Shiraia bambusicola*. *Ultrason Sonochem*. 2017;38:214–24.
26. Wang JW, Zheng LP, Zhang B, Zou T. Stimulation of artemisinin synthesis by combined cerebroside and nitric oxide elicitation in *Artemisia annua* hairy roots. *Appl Microbiol Biotechnol*. 2009;85:285–92.
27. Yang HL, Wang Y, Zhang ZB, Yan RM, Zhu D. Whole-genome shotgun assembly and analysis of the genome of *Shiraia* sp. strain Sif14, a novel endophytic fungus producing huperzine A and hypocrellin A. *Genome Announce*. 2014;2:e00011–4.
28. Ren XY, Liu YX, Tan YM, Huang YH, Liu ZY, Jiang XL. Sequencing and functional annotation of the whole genome of *Shiraia bambusicola*. *G3 Genes Genomes Genet*. 2020;10:23–35.
29. Zhao N, Li D, Guo BJ, Tao X, Lin X, Yan SZ, et al. Genome sequencing and analysis of the hypocrellin-producing fungus *Shiraia bambusicola* S4201. *Front Microbiol*. 2020;11:643.
30. Ganjewala D, Bob S, Raghavendra AS. Sodium nitroprusside affects the level of anthocyanin and flavonol glycosides in pea (*Pisum sativum* L. cv Arkel) leaves. *Acta Biol Szegediensis*. 2008;52:301–5.
31. Khezerluo M, Hosseini B, Amiri J. Sodium nitroprusside stimulated production of tropane alkaloids and antioxidant enzymes activity in hairy root culture of *Hyoscyamus reticulatus* L. *Acta Biol Hung*. 2018;69:437–48.
32. Zhao YX, Lim JY, Xu JY, Yu JH, Zheng WF. Nitric oxide as a developmental and metabolic signal in filamentous fungi. *Mol Microbiol*. 2020;113:872–82.
33. Zhang Y, Shi HB, Liang S, Ning GA, Xu NC, Lu JP, et al. *MoARG1*, *MoARG5*, *MoARG7* involved in arginine biosynthesis are essential for growth, conidiogenesis, sexual reproduction, and pathogenicity in *Magnaporthe oryzae*. *Microbiol Res*. 2015;180:11–22.
34. Dong JF, Zhang M, Lu L, Sun LN, Xu MJ. Nitric oxide fumigation stimulates flavonoid and phenolic accumulation and enhances antioxidant activity of mushroom. *Food Chem*. 2012;135:1220–5.
35. Sun CX, Ma YJ, Wang JW. Improved hypocrellin A production in *Shiraia bambusicola* by light-dark shift. *J Photochem Photobiol B Biol*. 2018;182:100–7.
36. Ma YJ, Sun CX, Wang JW. Enhanced production of hypocrellin A in submerged cultures of *Shiraia bambusicola* by red light. *Photochem Photobiol*. 2019;95:812–22.
37. Du W, Liang ZQ, Zou X, Han YF, Liang JD, Yu JP, et al. Effects of microbial elicitor on production of hypocrellin by *Shiraia bambusicola*. *Folia Microbiol*. 2013;58:283–9.
38. Besson-Bard A, Pugin A, Wendehenne D. New insights into nitric oxide signaling in plants. *Annu Rev Plant Biol*. 2008;59:21–39.
39. Zheng LP, Zhang B, Zou T, Chen ZH, Wang JW. Nitric oxide interacts with reactive oxygen species to regulate oligosaccharide-induced artemisinin biosynthesis in *Artemisia annua* hairy roots. *J Med Plants Res*. 2010;4:758–66.
40. Iigusa H, Yoshida Y, Hasunuma K. Oxygen and hydrogen peroxide enhance light-induced carotenoid synthesis in *Neurospora crassa*. *FEBS Lett*. 2005;579:4012–6.
41. Ponts N, Pinson-Gadail L, Verdal-Bonnin MN, Barreau C, Richard-Forget F. Accumulation of deoxynivalenol and its 15-acetylated form is significantly modulated by oxidative stress in liquid cultures of *Fusarium graminearum*. *FEMS Microbiol Lett*. 2006;258:102–7.
42. Reverberi M, Gazzetti K, Punelli F, Scarpari M, Zjalic S, Ricelli A, et al. *Aoyap1* regulates OTA synthesis by controlling cell redox balance in *Aspergillus ochraceus*. *Appl Microbiol Biotechnol*. 2012;95:1293–304.
43. Zhao N, Lin X, Qi SS, Luo ZM, Chen SL, Yan SZ. *De novo* transcriptome assembly in *Shiraia bambusicola* to investigate putative genes involved in the biosynthesis of hypocrellin A. *Int J Mol Sci*. 2016;17:311.
44. Hu JY, Sarrami F, Li H, Zhang GZ, Stubbs KA, Lacey E, et al. Heterologous biosynthesis of elsinochrome A sheds light on the formation of the photosensitive perylenequinone system. *Chem Sci*. 2019;10:1457–65.
45. Deng HX, Gao RJ, Liao XR, Cai YJ. Genome editing in *Shiraia bambusicola* using CRISPR-Cas9 system. *J Biotechnol*. 2017;259:228–34.
46. Li D, Zhao N, Guo BJ, Lin X, Chen SL, Yan SZ. Genetic overexpression increases production of hypocrellin A in *Shiraia bambusicola* S4201. *J Microbiol*. 2019;57:154–62.
47. Meraj TA, Fu JY, Raza MA, Zhu CY, Shen QQ, Xu DB, Wang Q. Transcriptional factors regulate plant stress responses through mediating secondary metabolism. *Genes*. 2020;11:346.
48. Beseli A, Amnuaykanjanasin A, Herrero S, Thomas E, Daub ME. Membrane transporters in self resistance of *Cercospora nicotianae* to the photoactivated toxin cercosporin. *Curr Genet*. 2015;61:601–20.
49. Ma YJ, Zheng LP, Wang JW. Bacteria associated with *Shiraia* fruiting bodies influence fungal production of hypocrellin A. *Front Microbiol*. 2019;10:2023.
50. Yao LY, Zhu YX, Jiao RH, Lu YH, Tan RX. Enhanced production of fumigaclavine C by ultrasound stimulation in a two-stage culture of *Aspergillus fumigatus* CY018. *Bioresour Technol*. 2014;159:112–7.
51. Turrion-Gomez JL, Benito EP. Flux of nitric oxide between the necrotrophic pathogen *Botrytis cinerea* and the host plant. *Mol Plant Pathol*. 2011;12:606–16.
52. Thevissen K, Terras FRG, Broekaert WF. Permeabilization of fungal membranes by plant defensins inhibits fungal growth. *Appl Environ Microbiol*. 1999;65:5451–8.
53. You BJ, Lee MH, Tien N, Lee MS, Hsieh HC, Tseng LH, et al. A novel approach to enhancing ganoderic acid production by *Ganoderma lucidum* using apoptosis induction. *PLoS ONE*. 2013;8:e53616.
54. Wu YX, Tiedemann AV. Impact of fungicides on active oxygen species and antioxidant enzymes in spring barley (*Hordeum vulgare* L.) exposed to ozone. *Environ Pollut*. 2002;116:37–47.
55. Pan WS, Zheng LP, Tian H, Li WY, Wang JW. Transcriptome responses involved in artemisinin production in *Artemisia annua* L. under UV-B radiation. *J Photochem Photobiol B Biol*. 2014;140:292–300.
56. Aebi H. Catalase in vitro. *Method Enzymol*. 1984;105:121–6.
57. Marklund S, Marklund G. Involvement of the superoxide anion radical in the autoxidation of pyrogallol and a convenient assay for superoxide dismutase. *Eur J Biochem*. 1974;47:469–74.
58. Tongul B, Tarhan L. The effect of menadione-induced oxidative stress on the *in vivo* reactive oxygen species and antioxidant response system of *Phanerochaete chrysosporium*. *Process Biochem*. 2014;49:195–202.

59. Lu CS, Ma YJ, Wang JW. Lanthanum elicitation on hypocrellin A production in mycelium cultures of *Shiraia bambusicola* is mediated by ROS generation. *J Rare Earth*. 2019;37:895–902.
60. Liu B, Bao JY, Zhang ZB, Yan RM, Wang Y, Yang HL, et al. Enhanced production of perylenequinones in the endophytic fungus *Shiraia* sp Sif14 by calcium/calmodulin signal transduction. *Appl Microbiol Biotechnol*. 2018;102:153–63.
61. Ma YJ, Lu CS, Wang JW. Effects of 5-azacytidine on growth and hypocrellin production of *Shiraia bambusicola*. *Front Microbiol*. 2018;9:2508.
62. Mortazavi A, Williams BA, McCue K, Schaeffer L, Wold B. Mapping and quantifying mammalian transcriptomes by RNA-Seq. *Nat Methods*. 2008;5:621–8.
63. Zhang J, Zhu LY, Chen HY, Li M, Zhu XJ, Gao Q, et al. A polyketide synthase encoded by the gene *An15g07920* is involved in the biosynthesis of ochratoxin A in *Aspergillus niger*. *J Agric Food Chem*. 2016;64:9680–8.

Publisher's Note

Springer Nature remains neutral with regard to jurisdictional claims in published maps and institutional affiliations.

Ready to submit your research? Choose BMC and benefit from:

- fast, convenient online submission
- thorough peer review by experienced researchers in your field
- rapid publication on acceptance
- support for research data, including large and complex data types
- gold Open Access which fosters wider collaboration and increased citations
- maximum visibility for your research: over 100M website views per year

At BMC, research is always in progress.

Learn more biomedcentral.com/submissions

